Biochemical and Biophysical Research Communications 375 (2008) 59–62

Contents lists available at ScienceDirect

Biochemical and Biophysical Research Communications

journal homepage: www.elsevier.com/locate/ybbrc

O-GlcNAcylation modulates the self-aggregation ability of the fourth microtubule-binding repeat of tau

Chun-Hui Yu [b,a], Tong Si [a], Wei-Hui Wu [a], Jia Hu [a], Jin-Tang Du [a], Yu-Fen Zhao [a], Yan-Mei Li [a,*]

[a] *Key Laboratory of Bioorganic Phosphorus Chemistry & Chemical Biology (Ministry of Education), Department of Chemistry, Tsinghua University, Beijing 100084, PR China*
[b] *Department of Chemistry, Beihua University, Jilin 132013, PR China*

ARTICLE INFO

Article history:
Received 21 July 2008
Available online 29 July 2008

Keywords:
Alzheimer's disease
Tau
Microtubule-binding repeat
Aggregation
O-GlcNAcylation

ABSTRACT

In Alzheimer's disease (AD), tau protein is abnormally hyperphosphorylated and aggregated into paired helical filaments (PHFs). It was discovered recently that tau is also *O*-GlcNAcylated in human brains. And *O*-GlcNAcylation may regulate phosphorylation of tau in a site-specific manner. In this work, we focused on the fourth microtubule-binding repeat (R4) of tau, which has an *O*-GlcNAcylation site—Ser356. The aggregation behavior of this repeat and its *O*-GlcNAcylated form was investigated by turbidity, precipitation assay and electron microscopy. In addition, conformations of these two peptides were analyzed with circular dichroism (CD). Our results revealed that *O*-GlcNAcylation at Ser356 could greatly slow down the aggregation speed of R4 peptide. This modulation of *O*-GlcNAcylation on tau aggregation implies a new perspective of tau pathology.

There are two hallmarks in Alzheimer's disease (AD): senile plaques and neurofibrillary tangles (NFTs) [1]. NFTs are aggregations of paired helical filaments (PHFs), which are mainly comprised of abnormally phosphorylated tau [2–4]. Tau protein is abundant in both central and peripheral nervous systems. The main function of tau is to stimulate and stabilize microtubule assembly from tubulin subunits [5]. It binds to microtubules with the microtubule-binding domain (MBD). The MBD contains four copies of a highly conserved 18-amino acid repeat, namely, R1, R2, R3, and R4. These repeats are separated from each other by a less conserved 13- or 14-amino acid inter-repeat (IR) domains [6]. Although tau protein is water-soluble and shows little tendency to aggregate under physiological conditions, it dissociates from microtubule and aggregates into PHFs in the brains of AD patients [7,8]. In the process of tau aggregation, the microtubule-binding domains are believed to play critical roles [9–12]. As aggregation of tau leads to toxicity in neurons, it is important to clarify the aggregation mechanism and develop a way to prevent this pathological aggregation.

It was discovered recently that tau protein was modified by *O*-GlcNAcylation (*O*-GlcNAc) in human brains [13]. *O*-GlcNAc is a type of protein *O*-glycosylation, by which the monosaccharide β-*N*-acetylglucosamine (GlcNAc) attaches to serine/threonine residues via an *O*-linked glycosidic bond [13]. For the *O*-GlcNAc, it was suggested that the sugar residue might transiently block phosphorylation site [14], or directly be involved in receptor binding interaction. And it might also alter the conformation of the peptide backbone [15,16]. In Alzheimer's disease, abnormal phosphorylation is believed to contribute to the conformation change and aggregation of tau protein [17–23]. However, whether and how *O*-GlcNAc is involved in the modulation of PHFs formation is not clear.

Ser356, located in the fourth microtubule-binding repeat (R4), is both the abnormal phosphorylation site [24] and the *O*-GlcNAcylation site [13] in tau protein. Furthermore, it is reported that *O*-GlcNAc might negatively regulate phosphorylation at Ser356 *in vivo* [13]. Our group has reported that R4 repeat is able to self-aggregate *in vitro*, and phosphorylation at Ser356 can modulate this process [19]. In this study, we focus on the effect of *O*-GlcNAc on the aggregation behavior of R4. Since different *O*-GlcNAc sites may have different effects on filament formation, it is advantageous to study the effect of only one confined *O*-GlcNAcylation site on a tau peptide. On the other hand, analysis of the effect of *O*-GlcNAc at defined sites is hampered by the low specificity of protein kinases and the highly dynamic turnover of *O*-GlcNAc *in vivo*. So we employed the synthetic *O*-GlcNAcylated peptide in our study.

In this study, peptide R4 and its *O*-GlcNAcylated form gR4 of the human tau protein (Table 1) were synthesized using the solid phase synthetic strategy. The conformational differences between R4 and gR4 were analyzed using circular dichroism (CD). The aggregation behavior of R4 and gR4 was examined by turbidity, precipitation assay, and electron microscopy. The results showed that *O*-GlcNAc at Ser356 negatively regulated the self-aggregation of R4 peptide.

* Corresponding author. Fax: +86 10 62781695.
E-mail address: liym@mail.tsinghua.edu.cn (Y.-M. Li).

0006-291X/$ - see front matter © 2008 Elsevier Inc. All rights reserved.
doi:10.1016/j.bbrc.2008.07.101

Table 1
Synthetic peptides corresponding to the fourth repeat domain of the human tau441 sequence

Tau peptide	Sequence amino acids	Repeat number
R4	V Q S K I G S L D N I T H V P G G G	350–367/fourth repeat
gR4	V Q S K I G gS L D N I T H V P G G G	350–367/fourth repeat

The subscripted g stands for *O*-GlcNAcylation.

Materials and methods

Peptide synthesis. Peptides were synthesized on Fmoc-Wang resin using the standard Fmoc/tBu chemistry and *O*-benzotriazol-*N*,*N*,*N*′,*N*′-tetramethyluronium hexafluorophosphate/1-hydroxybenzotriazol (HBTU/HOBt) protocol [25]. The amino acids were commercially available except for Fmoc-Ser(Ac_3-β-*O*-GlcNAc)-OH, which was prepared by a literature procedure [16]. The peptides and all protecting groups except the *O*-acetyl groups on the *N*-acetyl glucosamine were cleaved from the resin with TFA containing phenol (5%), thioanisole (5%), ethanedithiol (2.5%), and water (5%) for 120 min [26]. The crude peptides were purified by reverse-phase HPLC by using an ODS-UG-5 column (Develosil) with a linear gradient of 20–50% acetonitrile containing 0.06% trifluoroacetic acid as an ion-pairing reagent. Purified OG-peptide with acetyl-protecting GlcNAc$(OAc)_3$ was deprotected by 0.1 M NaOMe in methanol and finally purified by SepPak-C_{18} column. The integrity of each peptide was verified by ESI-MS. The sequences of the synthetic peptides are listed in Table 1.

Circular dichroism. The peptides (200 μM) were dissolved in phosphate buffer, pH 7.4, (10.0 mM Na_2HPO_4). CD spectra were recorded on a Jasco model J-715 spectropolarimeter (JASCO, Tokyo, Japan) at 298 K under a constant flow of nitrogen gas. Typically a quartz cell with a 0.1 cm path length was used for spectra recorded between 190 and 250 nm with a 1-nm scan interval. CD intensities reported in the figure are expressed in mdeg.

Monitoring of aggregation of R4 and gR4 by turbidity. The peptides (200 μM) were dissolved in PBS buffer, (137.0 mM NaCl, 3.0 mM KCl, 10.0 mM Na_2HPO_4, and 2.0 mM KH_2PO_4, ionic strength ~160.0 mM, pH 7.4). The same method was used to prepare peptide samples utilized for electron microscopy and precipitation assay. To study aggregation, peptides (200 μM) were incubated at room temperature in a nonbinding surface 96-well plate. The aggregation was monitored each day at the same time via turbidity measurements at 405 nm on Wellscan MK3 instrument (Labsystems Dragon Co., MA, USA).

Precipitation assay for peptide aggregation. Peptides (200 μM, dissolved in PBS buffer) were incubated at room temperature in 1.5 mL Eppendorf tubes. At the same time each day, the solutions were centrifuged (12,000*g*, 4 °C, 0.5 h) to precipitate insoluble filaments. The concentrations of peptides in supernatant were determined by UV absorption at 214 nm. UV measurements were performed on HP 8453 spectrophotometer (Hewlett Packard, USA) using quartz cuvettes (1-cm light path).

Transmission electron microscopy. Filaments were viewed by electron microscopy. Negative staining of the sample was performed on formvar- and carbon-coated 300-mesh copper grids. Samples were loaded on the grid and left for 2 min for absorption and then stained with 1% tungstophosphoric acid for another 2 min. After drying in a desiccator overnight, the samples were viewed on a JEOL-1200EX electron microscope (JEOL, Japan) at 100 kV.

Statistical analysis. The results are expressed as mean values ± SD, $n > 3$. Multiple comparisons were performed using Student's *t*-test, and differences with $p < 0.05$ were considered significant, and with $p < 0.01$ were considered very significant.

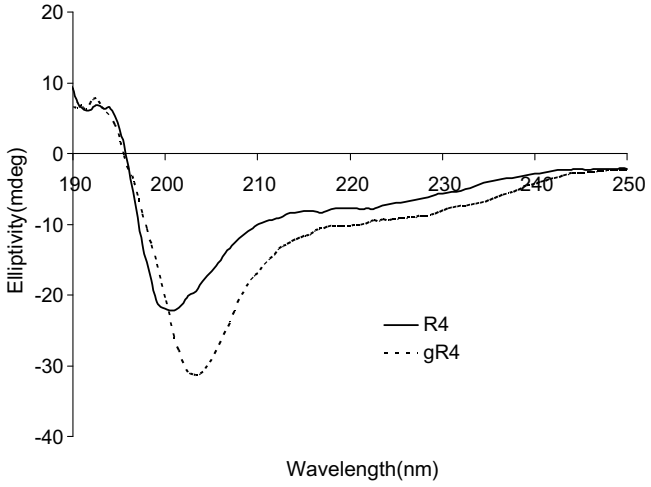

Fig. 1. Circular dichroism (CD) spectra of peptide R4 and glycopeptide gR4.

Results

O-GlcNAc at Ser356 induced conformational change in peptide R4

To study the conformations of the R4 and gR4 peptides, CD spectra was obtained in the region of 190–250 nm in aqueous solution (Fig. 1). The CD spectra for peptide R4 is characterized by a strong negative apex at 201 nm, and a flat-like pattern around a small negative apex at 221 nm. This indicated that there were some α-helical structure and a large amount of random coil [27]. On the other hand, gR4 peptide produced a different spectra pattern. *O*-GlcNAc at Ser356 shifted the strong negative apex from 201 to 204 nm. This difference showed that *O*-GlcNAc slightly altered the conformation of the peptide backbone. However, no remarkable structural changes were induced by *O*-GlcNAc.

Effect of O-GlcNAc on R4 aggregation

Aggregating study was performed in PBS, a buffer widely used to mimic the physiological condition [28,29]. Electron microscopy,

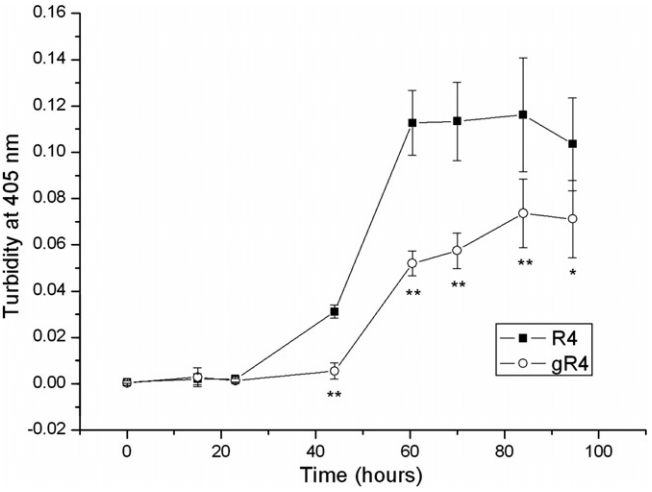

Fig. 2. The aggregation course of peptide R4 and glycopeptide gR4 as monitored by turbidity. Peptides were dissolved in PBS, pH 7.4, to a final concentration of 200 μM and incubated at room temperature. The assembly time course of peptide R4 and glycopeptide pR4 is plotted versus the incubation time according to the turbidity at 405 nm. The values are means ± SD, $n = 6$ replicate wells, from a single microplate. $^{*}P < 0.05$, $^{**}P < 0.01$ (Student's *t*-test).

turbidity, and precipitation assay all corroborate that both peptide R4 and glycopeptide gR4 are able to self-aggregate.

The kinetic process of aggregation was monitored by the time-dependent turbidity assay at 405 nm. As shown in Fig. 2, both R4 and gR4 exhibited the typical aggregation course, which had a short lag phase followed by rapid aggregation and eventually reached a plateau. However, the lag phase of R4 lasted for 23 h, which was 21 h shorter than that of gR4. This indicated that the nucleation of peptide R4 is considerably easier than that of glycopeptide gR4. Furthermore, at the plateau phase, the turbidity of R4 was significantly higher than gR4. This showed that the aggregation of R4 reached a higher final degree.

Precipitation assay was employed to assess the time-dependent formation of insoluble filaments [30] (Fig. 3). As shown in Fig. 3, after a lag phase, the peptide concentration in supernatant of R4 decreased sharply, which showed that R4 aggregated into insoluble filaments in a nucleation–elongation pattern. However, the concentration of gR4 in supernatant remained unchanged during 95 h. This indicated that, unlike R4, gR4 formed aggregates which could not be precipitated by the centrifugation at 12,000g. To sum up, precipitation assay demonstrated that R4 and gR4 formed different kinds of aggregates.

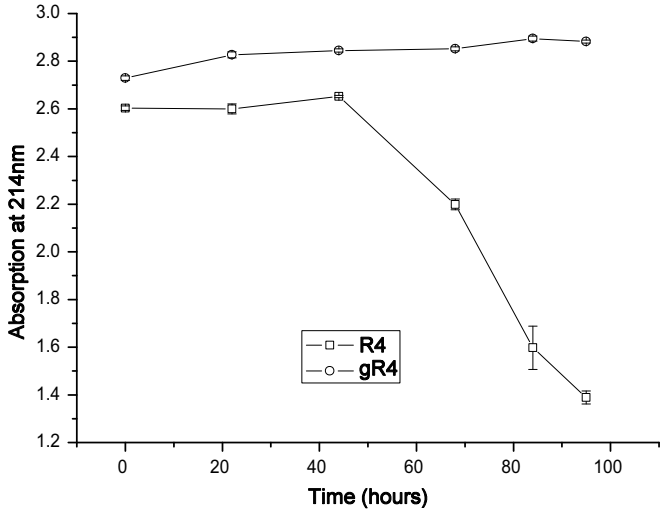

Fig. 3. Precipitation assay for filaments formation. R4 and gR4 were dissolved in PBS, pH 7.4, to a final concentration of 200 μM and incubated at room temperature. The solutions were centrifuged (12,000g, 4 °C, 0.5 h) to precipitate insoluble filaments. The concentrations of peptides in supernatant were determined by UV absorption at 214 nm. The values are means ± SD, $n = 3$.

The result of electron microscopy showed that, in contrast to the typical long filament of peptide R4, glycopeptide gR4 formed some shorter and thinner filaments (Fig. 4). Transmission electron microscopy confirmed that *O*-GlcNAc at Ser356 also modulated the filament form of R4 peptide.

Discussion

Emerging data indicates that *O*-GlcNAcylation may play an important role in Alzheimer's disease [31,32]. Recently, it is reported that tau is modified by *O*-GlcNAcylation in human brains. Whereas the effects of phosphorylation on the conformation and aggregation of tau protein have been intensely studied, little is known about the role of *O*-GlcNAc on aggregation behavior of tau. In this study, *O*-GlcNAc at Ser356 significantly slowed down the nucleation and aggregation speed of peptide R4. This modulating effect of *O*-GlcNAc on aggregation of the tubulin-binding motif might offer some clues on its role in AD. The negative regulation of *O*-GlcNAc on tau aggregation might be physiologically protective *in vivo*.

The different aggregation behavior of peptide R4 and glycopeptide gR4 might be explained by the different conformations of R4 and gR4. As seen from the CD spectra, *O*-GlcNAc had somewhat altered the conformation of R4 peptide. However, no remarkable conformational change was induced by *O*-GlcNAc. Then how does *O*-GlcNAc modulate the aggregation behavior of peptide R4? A possible explanation is that *O*-GlcNAc might affect the kinetics of conversion of the native structure to a filament-like structure [33]. In other words, *O*-GlcNAc might alter the structural proclivity among different conformational states, which results in different aggregation behavior.

In conclusion, we have demonstrated that R4 repeat of tau is capable of self-aggregation and *O*-GlcNAc at Ser356 can slow down the process of aggregation *in vitro*. These results imply that *O*-GlcNAcylation at Ser356 might serve as an aggregation regulator in the progression of Alzheimer's disease. This study may be valuable

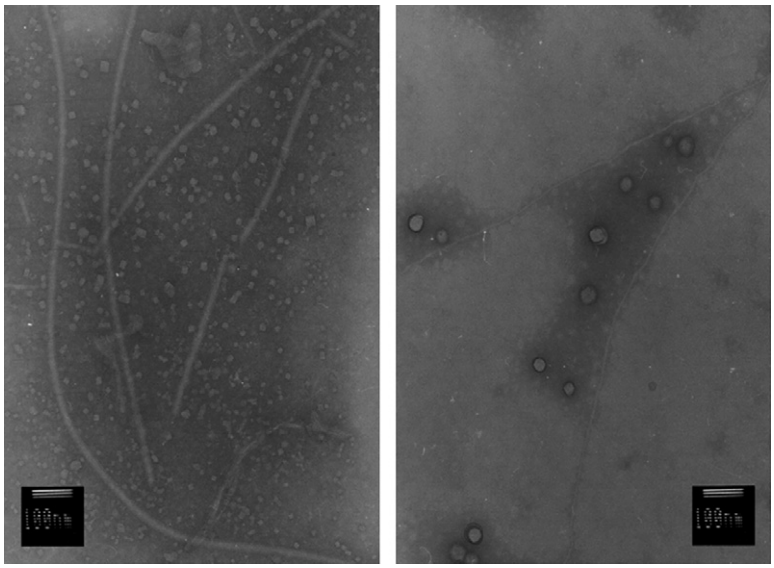

Fig. 4. Electron microscopy images of *in vitro* filaments of peptide R4 (left) and glycopeptide gR4 (right). The black bar in the figure represents 100 nm.

in future research to clarify the role of *O*-GlcNAcylation in Alzheimer's disease and other tauopathies.

Acknowledgments

The authors thank the financial support from National Natural Science Foundation of China (Nos. 20672067, 20532020) and National Undergraduate Innovation Training Project.

References

[1] E. Mandelkow, Alzheimer's disease—the tangled tale of tau, Nature 402 (1999) 588–589.
[2] Y.C.T.E. Kopke, S. Shaikh, A.C. Alonso, K. Iqbal, I. Grundke-Iqbal, Microtubule associated protein tau: abnormal phosphorylation of a non-paired helical filament pool in Alzheimer disease, J. Biol. Chem. 268 (1993) 24374–24384.
[3] I. Grundke-Iqbal, K. Iqbal, M. Quinlan, Y.C. Tung, M.S. Zaidi, H.M. Wisniewski, Microtubule-associated protein tau a component of Alzheimer paired helical filaments, J. Biol. Chem. 261 (1986) 6084–6089.
[4] I. Grundke-Iqbal, K. Iqbal, Y.C. Tung, M. Quinlan, H.M. Wisniewski, L.I. Binder, et al., Abnormal phosphorylation of the microtubule-associated protein τ (tau) in Alzheimer cytoskeletal pathology, Proc. Natl. Acad. Sci. USA 83 (1986) 49130–49170.
[5] C.X. Gong, F. Liu, I. Grundke-Iqbal, K. Iqbal, Post-translational modifications of tau protein in Alzheimer's disease, J. Neural Transm. 112 (2005) 813–838.
[6] G. Lee, N. Cowan, M. Kirschner, The primary structure and heterogeneity of tau protein from mouse brain, Science 239 (1988) 285–288.
[7] L. Buee, T. Bussiere, V. Buee-Scherrer, A. Delacourte, P.R. Hof, Tau protein isoforms, phosphorylation and role in neurodegenerative disorders, Brain Res. Rev. 33 (2000) 95–130.
[8] P. Friedhoff, M. von Bergen, E.M. Mandelkow, E. Mandelkow, Structure of tau protein and assembly into paired helical filaments, Biochim. Biophys. Acta 1502 (2000) 122–132.
[9] P. Friedhoff, M. von Bergen, E.M. Mandelkow, P. Davies, E. Mandelkow, A nucleated assembly mechanism of Alzheimer paired helical filaments, Proc. Natl. Acad. Sci. USA 95 (1998) 15712–15717.
[10] H. Wille, G. Drewes, J. Biernat, E.-M. Mandelkow, E. Mandelkow, Alzheimer-like paired helical filaments and antiparallel dimers formed from microtubule-associated protein tau in vitro, J. Cell Biol. 118 (1992) 573–584.
[11] S. Hiraoka, T.M. Yao, K. Minoura, K. Tomoo, M. Sumida, T. Taniguchi, T. Ishida, Conformational transition state is responsible for assembly of microtubule-binding domain of tau protein, Biochem. Biophys. Res. Commun. 315 (2004) 659–663.
[12] K. Minoura, T.M. Yao, K. Tomoo, M. Sumida, M. Sasaki, T. Taniguchi, T. Ishida, Different associational and conformational behaviors between the second and third repeat fragments in the tau microtubule-binding domain, Eur. J. Biochem. 271 (2004) 545–552.
[13] F. Liu, K. Iqbal, I. Grundke-Iqbal, G.W. Hart, C.X. Gong, *O*-GlcNAcylation regulates phosphorylation of tau: a mechanism involved in Alzheimer's disease, Proc. Natl. Acad. Sci. USA 101 (2004) 10804–10809.
[14] L. Wells, K. Vosseller, G.W. Hart, Glycosylation of nucleocytoplasmic proteins: signal transduction and O-GlcNAc, Science 291 (2001) 2376–2378.
[15] W.G. Wu, L. Pasternack, D.H. Huang, K.M. Koeller, C.C. Lin, O. Seitz, C.H. Wong, Structural study on O-glycopeptides: glycosylation-induced conformational changes of O-GlcNAc, O-LacNAc, O-sialyl-LacNAc, and O-sialyl-lewis-X peptides of the mucin domain of MAdCAM-1, J. Am. Chem. Soc. 121 (1999) 2409–2417.
[16] E.E. Simanek, D.H. Huang, L. Pasternack, T.D. Machajewski, O. Seitz, D.S. Millar, H.J. Dyson, C.H. Wong, Glycosylation of threonine of the repeating unit of RNA polymerase II with beta-linked *N*-acetylglucosame leads to a turnlike structure, J. Am. Chem. Soc. 120 (1998) 11567–11575.
[17] J.T. Du, Y.M. Li, Q.F. Ma, W. Qiang, Y.F. Zhao, H. Abe, K. Kanazawa, X.R. Qin, R. Aoyagi, Y. Ishizuka, T. Nemoto, H. Nakanishi, Synthesis and conformational properties of phosphopeptides related to the human tau protein, Regul. Pept. 130 (2005) 48–56.
[18] L.X. Zhou, Z.Y. Zeng, J.T. Du, Y.F. Zhao, Y.M. Li, The self-assembly ability of the first microtubule-binding repeat from tau and its modulation by phosphorylation, Biochem. Biophys. Res. Commun. 348 (2006) 637–642.
[19] J.T. Du, C.H. Yu, L.X. Zhou, W.H. Wu, P. Lei, Y. Li, Y.F. Zhao, H. Nakanishi, Y.M. Li, Phosphorylation modulates the local conformation and self-aggregation ability of a peptide from the fourth tau microtubule-binding repeat, FEBS J. 274 (2007) 5012–5020.
[20] A.D. Alonso, T. Zaidi, M. Novak, I. Grundke-Iqbal, K. Iqbal, Hyperphosphorylation induces self-assembly of tau into tangles of paired helical filaments/straight filaments,Proc. Natl. Acad. Sci. USA 98 (2001) 6923–6928.
[21] C. Haase, J.T. Stieler, T. Arendt, M. Holzer, Pseudophosphorylation of tau protein alters its ability for self-aggregation, J. Neurochem. 88 (2004) 1509–1520.
[22] C. Bancher, C. Brunner, H. Lassmann, H. Budka, K. Jellinger, G. Wiche, F. Seitelberger, I. Grundke-Iqbal, H.M. Wisniewski, Accumulation of abnormally phosphorylated tau precedes the formation of neurofibrillary tangles in Alzheimer's disease, Brain Res. 856 (2000) 163–175.
[23] W. Gordon-Krajcer, L.S. Yang, H. Ksiezak-Reding, Conformation of paired helical filaments blocks dephosphorylation of epitopes shared with fetal tau except Ser199/202 and Ser202/Thr205, Brain Res. 856 (2000) 163–175.
[24] J.M. Litersky, G.V.W. Johnson, R. Jakes, M. Goedert, M. Lee, P. Seubert, Tau protein is phosphorylated by cyclic AMP-dependent protein kinase and calcium/calmodulin-dependent protein kinase II within its microtubule-binding domains at Ser-262 and Ser-356, Biochem. J. 316 (1996) 655–660.
[25] G.B. Fields, R.L. Noble, Solid phase peptide synthesis utilizing 9-fluorenylmethoxycarbonyl amino acids, Int. J. Pept. Protein Res. 35 (1990) 161–214.
[26] P.F. Muhlradt, M. Kiess, H. Meyer, R. Sussmuth, G. Jung, Isolation structure elucidation and synthesis of a macrophage stimulatory lipopeptide from *Mycoplasma fermentans* acting at picomolar concentration, J. Exp. Med. 185 (1997) 1951–1958.
[27] H.Q. Yi, J. Gruszczynska-Biegala, D. Wood, Z.F. Zhao, A. Zolkiewska, Cooperation of the metalloprotease disintegrin and cysteine-rich domains of ADAM12 during inhibition of myogenic differentiation, J. Biol. Chem. 280 (2005) 23475–23483.
[28] F. Scaramozzino, D.W. Peterson, P. Farmer, J.T. Gerig, D.J. Graves, J. Lew, TMAO promotes fibrillization and microtubule assembly activity in the C-terminal repeat region of tau, Biochemistry 45 (2006) 3684–3691.
[29] S. Barghorn, E. Mandelkow, Toward a unified scheme for the aggregation of tau into Alzheimer paired helical filaments, Biochemistry 41 (2002) 14885–14896.
[30] Takeshi Chiba, Yoshihisa Hagihara, Takashi Higurashi, Kazuhiro Hasegawa, Hironobu Naiki, Yuji Goto, Amyloid fibril formation in the context of full-length protein, J. Biol. Chem. 47 (2003) 47016–47024.
[31] G.W. Hart, M.P. Housley, C. Slawson, Cycling of O-linked beta-*N*-acetylglucosamine on nucleocytoplasmic proteins, Nature 446 (2007) 1017–1022.
[32] W.B. Dias, G.W. Hart, O-GlcNAc modification in diabetes and Alzheimer's disease, Mol. Biosyst. 3 (2007) 766–772.
[33] F.C. Liang, R.P.Y. Chen, C.C. Lin, K.T. Huang, S.I. Chan, Tuning the conformation properties of a peptide by glycosylation and phosphorylation, Biochem. Biophys. Res. Commun. 342 (2006) 482–488.